RHEOLOGY AND GLASSY DYNAMICS OF FOAMS

M. E. CATES AND P. SOLLICH

Department of Physics and Astronomy
University of Edinburgh
JCMB, Kings Buildings
Mayfield Road, Edinburgh EH9 3JZ, UK

Abstract. After a brief 'warm-up' discussion of osmotic pressure of foams, the basic phenomena of foam rheology are reviewed, focusing on linear viscoelastic spectra (elastic and loss moduli) with brief mention of nonlinear effects. Theoretical models for some of these properties are then described, starting with Princen's model for the elastic modulus G_0 of an ordered foam in two dimensions. There is a basic conflict between this model, which predicts a step-function onset of the modulus when droplets first contact at volume fraction $\phi = \phi_0$, and the experimental data (which show $G_0 \sim \phi - \phi_0$). The three dimensional ordered case is reviewed next, focusing on anharmonic deformation theory which predicts a logarithmic softening of the modulus near ϕ_0; this is still not soft enough to explain the observations. The 3D disordered case is then addressed; a combination of disorder and the anharmonic effect finally seems able to explain the data. We then consider the problem of the frequency-dependent loss modulus $G''(\omega)$ which describes dissipation in a foam. Somewhat alarmingly, the data suggest behaviour incompatible with linear response theory; reconciliation is possible if one invokes some very slow relaxation processes at timescales longer than experiment. We briefly describe the search for foam-specific slow relaxation mechanisms of surfactant and water transport, which so far has yielded no viable candidates. Since similar anomalies in $G''(\omega)$ are observed in several other systems, they are instead tentatively ascribed to a generic phenomenon: glassy dynamics. A recent model for the rheology of "soft glassy matter" is then reviewed; though phenomenological, this suggests that glassy dynamics may be a useful concept in foam rheology.

1. INTRODUCTION

In these lectures we examine the rheological properties of liquid/gas foams (froths) and liquid/liquid foams (dense emulsions). We treat the foam as an array of droplets in a continuous matrix, where the volume of each droplet is constant in time. This neglects the compressibility of the fluid in the droplets; this is a good approximation whenever the characteristic scale of Laplace pressures σ/R (with σ surface tension and R the mean droplet radius) is small compared to the bulk modulus of the fluid, which is usually the case even for a froth. It also neglects *coarsening effects* which lead the droplet volumes to change slowly over time.

1.1. OSMOTIC PRESSURE

As a warmup exercise, we recap ideas about the osmotic pressure in a foam. To measure such a pressure, a foam is compressed by a semipermeable membrane through which the continuous phase (which we take to be water) can pass, but not the droplet phase. The force per unit area which must be exerted on the membrane is the osmotic pressure Π_0, which depends on ϕ, the volume fraction of the *droplet* phase. (We stick to this notation in these notes although others are used elsewhere in this Volume.) Alternatively Π_0 can be viewed as a function of V, the volume of the compressed foam.

The osmotic pressure obeys $\Pi_0(\phi) = -\partial F/\partial V$ with the derivative taken at fixed number of droplets. To a very good approximation (which neglects the tiny translational entropy of the droplets), $F = \sigma A$ where $A(V)$ is the total surface area of the droplets. Hence $\Pi_0(\phi)$ is zero for $\phi < \phi_0$, where ϕ_0 is the threshold at which droplets first come into contact and start to deform. For higher volume fractions, the droplets develop flattened facets; these are small just above the threshold but soon become fully developed bilayer films as ϕ is further increased. The remaining water then resides in *Plateau borders* along the edges of the polyhedral droplets with further water pockets at the vertices.

2. BASIC RHEOLOGY

2.1. LINEAR VISCOELASTICITY

Linear viscoelastic theory describes the response of a material to small deformations. Consider, for example, an imposed simple shear through a strain angle γ (assumed small) suddenly imposed at time zero and then held constant. The resulting shear stress is

$$s(t) = \gamma G(t) \tag{1}$$

For a Hookean solid, $s = G_0\gamma$ and there is no time dependence; G_0 is the shear modulus of the material:

$$G_0 = \left(\frac{\partial^2 F}{\partial \gamma^2}\right)_V \tag{2}$$

For a Newtonian fluid, instead $s = \eta\dot{\gamma}$ where η is the viscosity. (Formally this corresponds to a delta-function transient for $G(t)$.) Viscoelastic solids show behaviour intermediate between these extremes, with a nontrivial transient in $G(t)$ followed by a plateau, $G(\infty) \to G_0$ at long times. Viscoelastic fluids are similar but there is either no plateau or else one which lasts a finite time before $G(t)$ finally decays to zero. Foams do show a well-developed plateau, of amplitude G_0 which we call the *plateau modulus*; they are usually viewed as viscoelastic solids.

A related experiment is oscillatory shear, $\gamma = \Re[\gamma_0 e^{i\omega t}]$, for which the stress is

$$s(t) = \Re[G^*(\omega)\gamma_0 e^{i\omega t}] \tag{3}$$

with $G^*(\omega) = G'(\omega) + iG''(\omega)$ where G', G'' are called the storage modulus and the loss modulus. These control respectively the in-phase (elastic) response and the out-of-phase (viscous) response, of the medium. Their ratio obeys $G''/G' = \tan\delta$ where $\delta(\omega)$ is the phase shift between the measured stress and the applied strain.

Linear response theory (see e.g. [1]) shows that

$$G^*(\omega) = i\omega \int_0^\infty G(t)e^{-i\omega t}\, dt \tag{4}$$

Since $G(t)$ is real, this requires that $G'(\omega) = G'(-\omega)$ whereas $G''(\omega) = -G''(\omega)$. Thus the loss modulus is an odd function of frequency which means that it *must vanish* as $\omega \to 0$.

2.2. FOAM PHENOMENOLOGY

Foam are found to have a well defined elastic modulus $G(t \to \infty) = G_0(\phi)$ which depends interestingly on the volume fraction ϕ, as well as on surface tension σ and (mean) droplet size R. Specifically, G_0 rises *smoothly* from zero as ϕ is raised above ϕ_0. Surprisingly perhaps, most theories cannot explain this, and below we discuss this problem in some detail.

According to linear response theory, the plateau modulus G_0 can also be measured as $G'(\omega \to 0)$; and in most foams a limiting value can readily be extracted from the frequency dependent spectra. However, there is a strongly anomalous behaviour in $G''(\omega)$, which, in apparent contradiction to linear response theory, does not vanish at low frequencies but instead

seems to approach a constant value or (in some cases) even to be rising as the frequency is lowered. (Typical G'' values at low frequency are between 1/5 and 1/50 of G_0.) This is a cause for concern, to which we return in Section 4.

2.3. NONLINEAR EFFECTS

These can arise when either the stress s or the strain γ is not small. In most foams one observes the phenomenon of *yielding*: if a stress s is maintained in steady state, then for $s < s_Y$ the material attains a finite deformation and then stops moving (finite γ) whereas for $s > s_Y$ the steady state motion involves finite $\dot{\gamma}$ and the sample deforms indefinitely (creep). This behaviour defines a steady-state *flow curve* which is a plot of stress against strain rate $\dot{\gamma}$. If the "yield stress" s_Y is nonzero (solid-like behaviour) the curve comprises a vertical line segment at $\dot{\gamma} = 0$ followed by a smooth continuation. Although many other nonlinear measurements are possible, in these lectures we avoid discussion of these. Moreover, up until Section 5, we will focus exclusively on *linear* viscoelastic phenomena.

3. THE ELASTIC MODULUS

3.1. PRINCEN'S MODEL

The simplest model [2, 3] for foam elasticity considers an array of cylindrical "droplets" in a two-dimensional ordered hexagonal packing. The geometry is shown in Fig. 1. We consider a sample of unit length into the page, in which case the free energy per cylinder is

$$F_{\rm cyl} = \sigma(6L + 2\pi r) \tag{5}$$

where $(6L + 2\pi r)$ is the perimeter of the cylinder, $L = a - 2r/\sqrt{3}$ the facet length, a the side of a hexagonal cell and r the radius of the Plateau borders.

The volume fraction ϕ is the ratio of the cross-sectional area of a droplet to that of the hexagonal cell

$$\phi = \frac{\pi R^2}{3\sqrt{3}a^2/2} \tag{6}$$

where R is the radius of a free (circular) cylindrical drop. The contact point ϕ_0 is fixed by requiring $a = 2R/\sqrt{3}$ and hence (after some algebra)

$$\frac{a}{R} = \frac{2}{\sqrt{3}}\left(\frac{\phi_0}{\phi}\right)^{1/2} \tag{7}$$

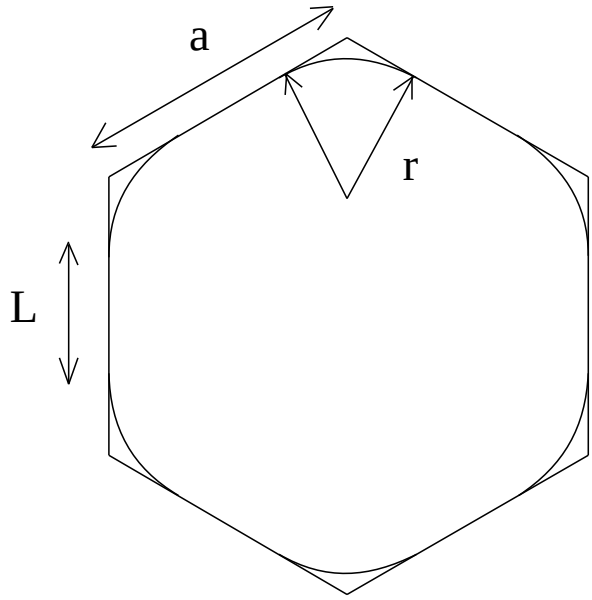

Figure 1. Geometry of a "droplet" in a two-dimensional ordered hexagonal foam.

and $\phi_0 = 0.91$. Likewise one finds

$$F_{\rm cyl} = 2\pi\sigma R\left[\frac{1}{\phi_0\phi} - \left(\frac{1-\phi_0}{\phi_0}\right)^{1/2}\left(\frac{1-\phi}{\phi}\right)^{1/2}\right] \tag{8}$$

which is completely fixed by geometry.

We first use this result to find the osmotic pressure $\Pi_0 = -(\partial F(V)/\partial V)_R$ where $F(V) = F_{\rm cyl}/\phi$:

$$\Pi_0 = \frac{\sigma}{R}\left[\left(\frac{1-\phi_0}{1-\phi}\right)^{1/2} - 1\right] \tag{9}$$

(This is shown in Fig. 2.) Note that $\Pi_0 \sim (\sigma/R)f(\phi)$ where f is a dimensionless function. According to the model, this function *vanishes smoothly* as $\phi \to \phi_0^+$ and diverges as $\phi \to 1$, when the Laplace pressure σ/r formally becomes infinite (since $r \to 0$). Both features are broadly confirmed by experiment [4, 5].

Turning now to the elastic modulus G_0, we must find the change in surface area of the droplets when the lattice is deformed. We choose for simplicity a shear direction parallel to the direction joining droplet centres, and note that by the Young-Laplace law, the 120^o angles between films (extrapolated through the border regions) are preserved on deformation;

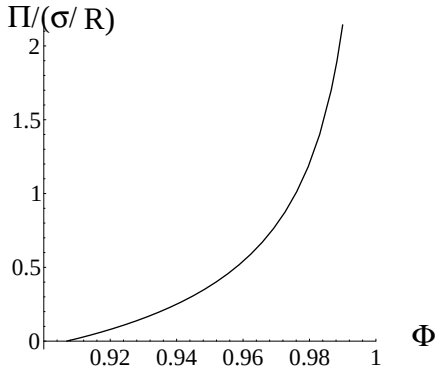

Figure 2. Osmotic pressure of a two-dimensional ordered hexagonal foam

otherwise there would be unbalanced forces on the borders. Each deformed droplet therefore occupies an irregular hexagon whose corners each contain one third of a plateau border (whose radius is still r). The resulting free energy per cylinder is

$$F_{\rm cyl} = 2\sigma\left[\pi r + L_1 + L_2 + L_3\right] \tag{10}$$

where $L_{1,2,3}$ are the film lengths, or equivalently

$$F_{\rm cyl}(\gamma) - F_{\rm cyl}(0) = 2\sigma\left[a_1 + a_2 + a_3 - 3a\right] \tag{11}$$

where $a_{1,2,3}$ are the sides of the deformed hexagonal cell. Notice that for given a, *this expression is independent of volume fraction.* In other words, the area change on deformation, which is entirely attributable to stretching of the film regions, does not depend on how large these films are originally – except that of course the calculation breaks down for $\phi < \phi_0$ when the films simply do not exist.

From this calculation one can find G_0 from the stored free energy using

$$F(V,\gamma) - F(V,0) = VG_0\gamma^2/2 \tag{12}$$

which holds in the limit of small strain γ. This gives the result

$$G_0 = \frac{\sigma}{\sqrt{3}} = \frac{\sigma}{2R}\left(\frac{\phi}{\phi_0}\right)^{1/2} = 0.525\frac{\sigma}{R}\phi^{1/2} \tag{13}$$

which has a finite value of $0.525\sigma/R$ as $\phi \to \phi_0^+$. Accordingly the Princen model predicts a *step discontinuity* in the elastic modulus G_0 at $\phi = \phi_0$.

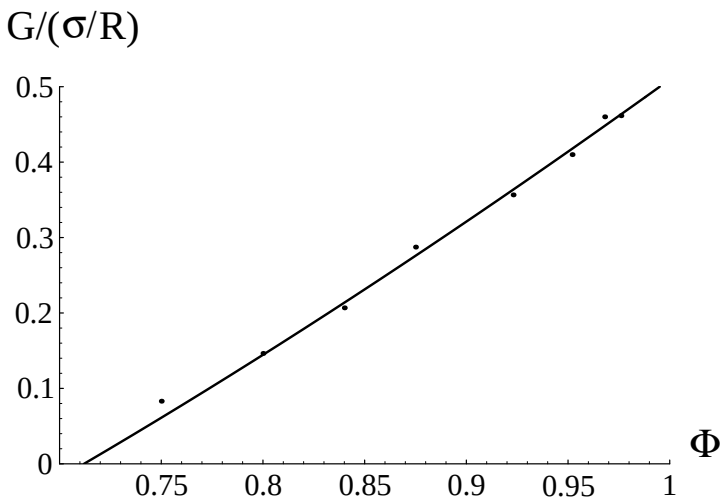

Figure 3. Shear modulus of a biliquid foam, from [4]. The solid line is a (semi-)empirical fit.

This contrasts with the prediction for osmotic pressure Π_0 (which rises linearly from zero) but is similar to that for the bulk modulus $B_0 = -\partial\Pi/\partial V$.

The step discontinuity is not consistent with experiments on either polydisperse [4] or near-monodisperse [5] foams: see Fig. 3. Candidates for explaining the discrepancy include: (a) the fact that real foams are three dimensional; (b) the fact that they are disordered; or, (c) some combination of these.

3.2. 3D ORDERED FOAMS

To find $G_0(\phi)$ for a three-dimensional foam is a hard task, because the Plateau borders have a more complex geometry (see other lectures in this volume!). There are three main approaches. The first is to guess the shape of the borders; so long as volume constraints are respected, the resulting surface will always have a larger area than the true one (which is the state of least free energy and hence minimal area). So the "guessing" method gives an upper bound on $F(V)$ and can in principle be refined systematically, for example by including variational parameters in the guessed shape, and minimizing the computed area over these parameters. However, in what follows, we shall follow Refs. [6, 7] and simply guess. The second line of attack involves an exact analysis for the limit $\phi \to \phi_0$ in which droplets are weakly compressed. This is informative since it addresses precisely the region where the Princen model fails to explain the data. Finally, numerical

approaches based on the surface evolver programme [8] can be used. We describe these aspects in turn.

Before doing this, however, we make a technical amendment to the calculation: it turns out to be much easier to calculate the *uniaxial elongation modulus*, $\mu_0(\phi)$, than the shear modulus $G_0(\phi)$. The former is defined by stretching a unit cube of material so that the lengths of its sides become $1+\epsilon$ along the stretch direction and $1-\epsilon/2+3\epsilon^2/8$ along the remaining two. (This deformation preserves volume.) In terms of the elongational strain ϵ, we have

$$F(V,\epsilon) - F(V,0) = V\mu_0(\phi)\epsilon^2/2 \tag{14}$$

which serves as the definition of μ_0. For an *isotropic material* such as a real foam, one can prove $G_0 = \mu_0/3$, whereas for an ordered array of droplets, both G_0 and μ_0 in principle are functions of orientation. So, given that results from an oriented model have to be compared with experimental data on an isotropic system, it is no less valid to compute $\mu_0(\phi)$ than $G_0(\phi)$. Moreover, at least for the purpose of qualitative comparison, one can choose the direction for our elongational distortion so as to minimise the algebra involved.

Buzza and Cates [6] performed such a calculation with a simple cubic array of droplets. Though in obvious violation of the Young Laplace condition, this allows even more algebraic simplification and should not *qualitatively* affect the nature of the singularity at $\phi \to \phi_0$ (i.e., smooth onset versus jump discontinuity). Their guess for the droplet shape was a truncated sphere: that is, the droplet surface is the inner envelope of the intersection between a sphere and the deformed (cubic) unit cell. To maintain constant droplet volume, the radius of the sphere must change as the unit cell is deformed (Fig. 4). Results for this model (Fig. 5) show a jump discontinuity at $\phi = \phi_0 = 0.52$, closely resembling that of the Princen model.

In the second approach to this problem, the limit of weak compression, $\phi \to \phi_0^+$ is addressed using the theory of Morse and Witten [9]. This is a perturbative treatment which exploits the fact that at weak compression, the droplet shape is almost spherical, with small faceted regions. Accordingly it can be studied by analysing the response of a spherical drop to a weak external force field. The latter induces pressure shifts on either side of the droplet surface, $p_{\rm out}(\Omega)$ (where Ω is an angle) and $p_{\rm in}$. The latter is an angle-independent quantity whose value is chosen to maintain constant volume for the droplet overall. In units where the free droplet radius R and surface tension σ are both unity, the Laplace equation reads

$$-(\nabla^2 + 2)\rho(\Omega) = p_{\rm in} - p_{\rm out}(\Omega) \tag{15}$$

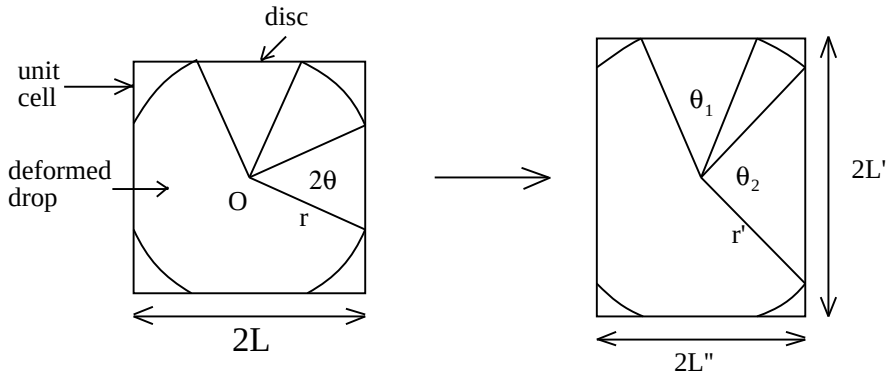

Figure 4. Truncated sphere model. Each droplet is modelled as a truncated sphere within a cubic unit cell. On uniaxial deformation the radius of the drop, as well as the geometry of the unit cell, are changed.

where the left hand side is the local curvature (the 2 comes from the reference shape of a sphere) and the right hand side is the local Laplace pressure across the interface. In this equation $\rho(\Omega)$ is the local (normal) displacement of the droplet surface.

Morse and Witten calculated the response function G determining the displacement field, $\rho(\Omega) = G(\Omega, \Omega')f$, in response to a point force $p_{\rm out}(\Omega) = f\delta(\Omega - \Omega')$. In terms of the angle θ between Ω and Ω', this reads:

$$G(\Omega, \Omega') = \frac{-1}{4\pi}\left[\frac{1}{2} + \frac{4}{3}\cos\theta + \cos\theta \ln\left(\sin^2(\theta/2)\right)\right] \qquad (16)$$

This allowed them to calculate the free energy of the weakly compressed droplet. For a small facet subject to a localised force f, they found a free energy contribution

$$\delta F = \frac{1}{8\pi} f^2 \left[-\ln(f/8\pi) - 4/3\right] \qquad (17)$$

This can be compared with Hooke's law for a spring of stiffness k, $\delta F = f^2/2k$, revealing that small facets act as *logarithmically soft* springs, having an effective spring constant $k_{\rm eff} \sim -1/\ln f$, which tends to zero as $f \to 0$.

The Morse-Witten effect can be incorporated into the simple cubic model of an emulsion to find a more accurate expression for the elastic modulus G_0 near onset (also shown in Fig. 5). Although this offers a formal improvement, in that the step discontinuity is replaced by a smooth curve, the slope at ϕ_0 remains infinite, and the prediction still has scant resemblance to the experimental data [4, 5].

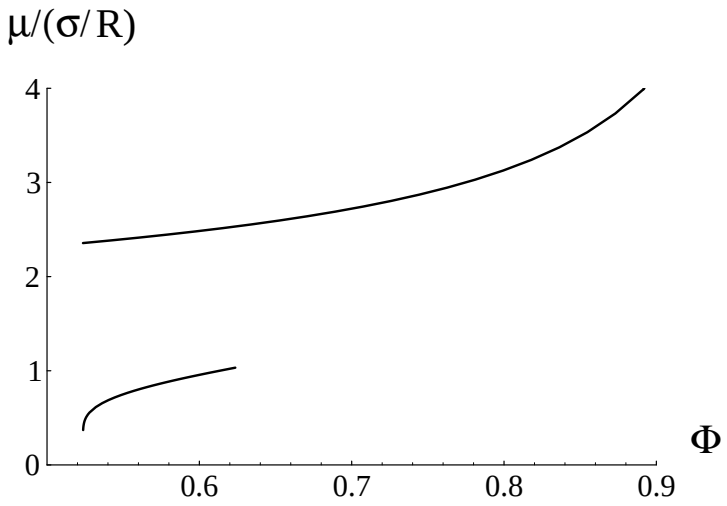

Figure 5. Results for the truncated sphere model (upper curve) and those incorporating the Morse-Witten correction for small compressions.

We now discuss the third approach to the problem of 3-D ordered foams: the numerical one. Lacasse, Grest and Levine [7] used the surface evolver [8] to study the free energy of spherical droplets squeezed into a series of n-faced polyhedra. The case $n = 2$ (a droplet between parallel plates) is an unrealistic but interesting limit, because the surface shape can then be found exactly using the calculus of variations. As well as benchmarking the surface-evolver calculations, the exact solution can be compared with the Morse-Witten theory (at small compressions) and also with the truncated sphere model. In fact, the truncated sphere model is never very good: at small compressions the Morse-Witten result is approached whereas at larger ones the data approach a model in which the droplet shape is a disc surrounded by a toroidal "bulge" of *semicircular* cross-section. (Such a bulge joins onto the films tangentially, unlike the truncated sphere, so it is not surprising that this gives a better result; however, the extension to $n > 2$ is not obvious.)

For larger n, the free energy data was found to be well fit by the empirical form

$$\delta F \simeq nC \left[\left(\frac{R}{h} \right)^3 - 1 \right]^\alpha \tag{18}$$

where $\alpha(n)$ varies between 2.1 ($n = 2$) and 2.6 ($n = 20$), and $C(n)$ between about 7 and about 70. Here R is the free droplet radius and h the perpendicular distance from the centroid of the polyhedron to the centre

of a face. Note that most of the n values correspond to shapes that do not tesselate in three space: this is probably not crucial since in reality n is not the same for all droplets in a foam. Note that because $\alpha > 2$, the model corresponds to a soft (power-law) spring interaction at contacting facets. Using the results for simple cubic and face-centered cubic unit cells, Lacasse et al. predicted the shear modulus and found curves rather similar to those found by Buzza and Cates using the Morse-Witten potential. In other words, they again found a smooth curve for $G_0(\phi)$, but with an infinite slope at $\phi = \phi_0$ rather than the finite slope seen experimentally.

3.3. ROLE OF DISORDER

This was studied in two dimensions by Hutzler and Weaire [10, 11], and Durian [12]. As emphasised long ago by Weaire and others, one would expect the disorder to wash out the step discontinuity, replacing it with a much smoother curve, and this indeed was seen computationally. However, it is difficult to perform accurate simulations very close to ϕ_0, and these authors did not get extremely close.

The three dimensional version was studied by Lacasse et al [13], without, however, including explicitly the details of the foam structure (thereby limiting the computational load). Instead an anharmonic pair potential was constructed by appeal to the findings quoted above for δF in polyhedral boxes:

$$U(d) = C\left[\left(\frac{2R}{d}\right)^3 - 1\right]^\alpha \tag{19}$$

where averaged parameters $\alpha = \alpha(\bar{n}) \simeq 2.3$ and $C = C(\bar{n})$ were chosen. Here d is the distance between droplet midpoints; the U's are summed over droplets within range $d < 2R$ (that is, summed over facets). This potential was fed into a very large MD simulation and the response to compression and shear distortions measured. Data for the shear modulus is compared with experiment in Fig. 6; that for the osmotic pressure is also in reasonable agreement. It appears that by combining disorder and anharmonicity, one finally gets close to the experimental behaviour; this certainly cannot be achieved using anharmonicity alone and arguably also cannot be achieved solely with disorder [14]. The significance of disorder was highlighted by a study of the individual droplet displacements under shear: these were found to be highly non-affine (in other words, different droplets moved in different directions).

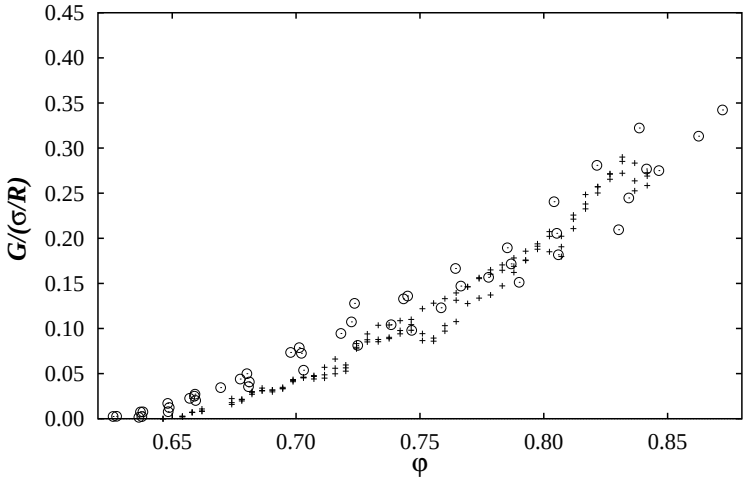

Figure 6. Shear modulus of a 3d foam found by simulation (+) [13] and experiment [5].

4. DISSIPATION IN FOAMS

Above we have described calculations of the linear elastic modulus $G_0 = G'(\omega \to 0)$. W now return to the problem of understanding the linear loss modulus, $G''(\omega)$, whose low frequency behaviour remains very puzzling. Specifically, it shows no sign of vanishing at low frequencies, instead remaining constant or even increasing as frequency is lowered.

The lowest frequencies easily accessed by experiment are of order 0.1 Hz. Hence the observed anomaly might be resolved if one could find relaxational modes of the foam having *characteristic frequencies* well below this. Candidates for such modes fall into two classes: *specific* relaxation mechanisms arising from the physics of films, Plateau borders, etc., which are restricted directly to foams; and *generic* mechanisms associated with more universal aspects of disorder. In this Section we restrict attention to the first type, and show that there are no really obvious candidates. In Section 5 we therefore review a recent model for generic dynamics in "soft glassy materials", which we believe may include foams.

4.1. QUALITATIVE ANALYSIS OF SLOW MODES

If there are slow relaxation modes in foams, the observed "low frequency" viscoelastic spectrum can be interpreted as shown schematically in Fig. 7. In other words, at still lower frequencies, relaxation modes would be seen, each causing a drop ΔG in $G'(\omega)$ and a bump in $G''(\omega)$ as the frequency is tracked downward. For a simple (Maxwell) process, the maximum

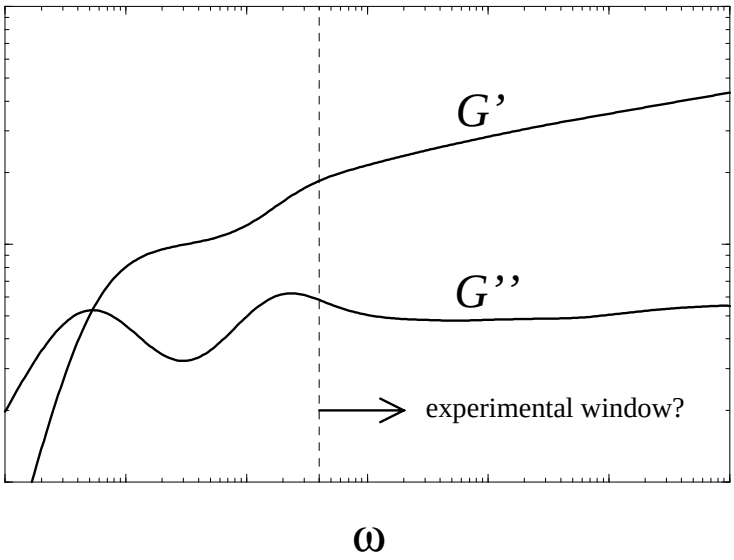

Figure 7. Sketch of viscoelastic spectrum, showing possible relaxations at frequencies below the measurement window.

height of the bump in G'' is also ΔG; for a distribution of relaxation times both the drop and the bump are smeared out. Given that G'' is an appreciable fraction (say 1/10) of G' at the measured frequencies, this explanation requires not only that the characteristic frequencies of the mode(s) be low (say < 0.1 Hz), but also that the corresponding amplitudes ΔG be a reasonable fraction of G_0.

The exact calculation of the relaxation modes is far beyond our present capabilities. However, qualitative estimates can be made by the following strategy. (i) Identify sources of dissipation and express these as steady state viscosities $\Delta\eta_i$; (ii) Identify the corresponding driving forces and express these as amplitudes ΔG_i (found from the excess stored free energy in the strained state); (iii) Construct the characteristic frequency as $\omega_i = \Delta G_i/\Delta\eta_i$. The following discussion summarises that of Buzza, Lu and Cates [15]. Numerical estimates are generally those appropriate to small-cell biliquid foams as studied by Mason, Weitz and Bibette [5], and dissipation estimates are quoted per unit volume.

4.2. SOURCES OF DISSIPATION

Consider first a wet foam. This has films of thickness d (so far neglected, but finite in practice), in equilibrium with borders of mean radius r. The Laplace pressure in the borders is balanced, within the water films, by the *disjoining pressure* Π_d. This arises from the direct interaction between the surfactant monolayers across the thin water film; without it, foams would not be stable. We assume that the wet foam has $R \gg r \gg d$ and that the borders provide a *good reservoir* of surfactant. That is, we assume that *static* changes in film surface area negligibly perturb the chemical potential of the surfactant in the foam. (Transient changes may however set up temporary gradients in the chemical potential.) Possible dissipation sources include the following.

Fluid viscosity: In most cases, this contribution is dominated by the shearing of the water films (as opposed to the fluid within droplets).

Diffusion resistance: If a diffusive current $\mathbf{j}$ of surfactant is driven relative to stationary water by a chemical potential gradient, there is an entropy production. This is precisely analogous to the Joule heating by electrons flowing down a wire from high to low chemical potential (voltage). An expression for the heat production is given later.

Intrinsic dissipation in monolayers: The surfactant monolayers are 2-D fluid films characterised by a shear viscosity μ and dilational viscosity κ. (In fact, several different κ's can be defined for films in different states of equilibrium with a reservoir; this is discussed in Ref. [15] but ignored here.) Rough estimates for μ are in the range $10^{-7} - 10^{-6}$ kg s^{-1} and for κ, about $10^{-6} - 10^{-4}$ kg s $^{-1}$, although the latter is hard to measure (and/or define).

4.3. DRIVING FORCES

Each driving force can be associated with a free energy contribution $\Delta F = V\Delta G\gamma^2/2$ which contributes to the elastic stress until such time as the stored free energy relaxes.

Gibbs elasticity: For example, the free energy increment in a stretched film is

$$\delta F = \sigma\delta A + E(\delta A)^2/2A \tag{20}$$

where E is the Gibbs elastic constant. As with κ, different E's can be defined depending on the state of equilibrium of the film; if it is instantaneous exchange contact with a surfactant reservoir, E is zero. But if the density of surfactant per unit area is reduced by a sudden expansion of the film, then a finite Gibbs elastic storage will occur until this transient density deficit is rectified (by surfactant diffusion or some other mechanism). The value of E used below refers to this situation.

Surface tension: We distinguish this from the surface tension *gradients* arising from Gibbs elasticity. The latter can become large, and may represent a stronger driving force than surface tension itself. Pure surface tension remains relevant, however, since it is what causes the relaxation of a nonminimal surface toward a minimal one, under conditions where the surfactant has reached equilibrium.

Disjoining pressure: This provides a third driving force, which drives the equilibration of the film thickness d to the proper value (at which it becomes balanced by Laplace pressure).

4.4. A THEOREM

To summarise the above, shear deformation requires currents of both water and surfactants to be set up in the foam, to transport these materials from their old to their new positions. The driving forces responsible are Gibbs elasticity (strong), surface tension (weaker) and disjoining pressure (weak, except in dry or nearly dry foams [15]) and the dissipations involve water viscosity, film viscosities, and diffusion resistance.

A theorem of nonequilibrium thermodynamics [16] states in essence that "If alternative pathways exist for relaxing the same driving force, the *least dissipative* is chosen". Note that this is only true strictly within the linear response regime – but that is enough for us. Versions of the theorem involve the well-known variational principles of least dissipation in Stokes equation of fluid motion and Kirchoff's laws for resistor networks. Accordingly, for qualitative purposes we should think of possible patterns of water and surfactant fluxes and choose the least dissipative. (This is a poor mans substitute for the full solution of the problem, which would involve finding the full equations of motion from a variational principle, and solving these explicitly.)

4.5. DRY LIMIT

It is easier to think of candidate flux patterns in the dry limit where the borders are not present; the film thickness d is, however, finite. Consider a hexagonal array under slow shearing: there are regions where films contract and others where they expand. In the contracting (expanding) regions there is too much (too little) of both water and surfactant. Considering the water current first, the required transport can arise via Poiseuille type flow of water with a film (Fig. 8). The associated dissipation rate (per unit volume) is of order $T\dot{S} = \eta_W R\dot{\gamma}^2/d$ as may be confirmed by checking the typical shear rate within a film ($\simeq \dot{\gamma}R/d$) and taking account of the film volume fraction ($\simeq d/R$). The driving force for this motion is essentially Π_d.

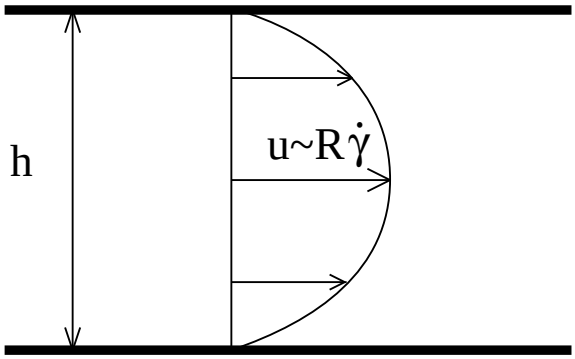

Figure 8. Poiseuille flow of water with a film of thickness h; the typical fluid velocity near the film centre is of order $R\dot{\gamma}$.

Because there is a nontrivial stress boundary condition at the surfactant monolayers, the mean velocity in the centre of a moving film is, according to this mechanism, larger than at the edges. Thus, although part of the surfactant is swept along with the water, this does not give the right surfactant flux overall. An obvious way to balance the flux is by diffusion of surfactant within the watery part of the films. For typical biliquid foams (where the surfactant concentration in this region is very small) this is extremely dissipative [15]: $T\dot{S} \simeq RT\dot{\gamma}^2/(dDc\Sigma^2)$ with D the surfactant diffusivity and Σ the area per molecule in a monolayer. (Note that this scales inversely with surfactant concentration.) So if a less dissipative route can be found, the system will choose it.

Such a route involves "Marangoni flow", that is, collective motion of the surfactant layers along the film surface (dragging some fluid along for the ride). Clearly, by combining this with the Poiseuille flow in some linear combination, the required ratio of surfactant to water fluxes can be achieved. Such a resultant flow is shown in Fig. 9: note, however, that to get a suitable overall flow pattern requires shearing within the *monolayers* as well as within the water; the dissipation is thus found to be $T\dot{S} \simeq \eta_W R\dot{\gamma}^2/d + k\dot{\gamma}^2/R$. The driving force for this motion is essentially Gibbs elasticity.

4.6. WET FOAM

For a wet foam, the preceding flow patterns are still possible, but an extra possibility arises. This is called *Marginal Regeneration* and involves the push/pulling of fully-formed bilayer films into and out of the Plateau border regions. There is then negligible dissipation within the body of the film,

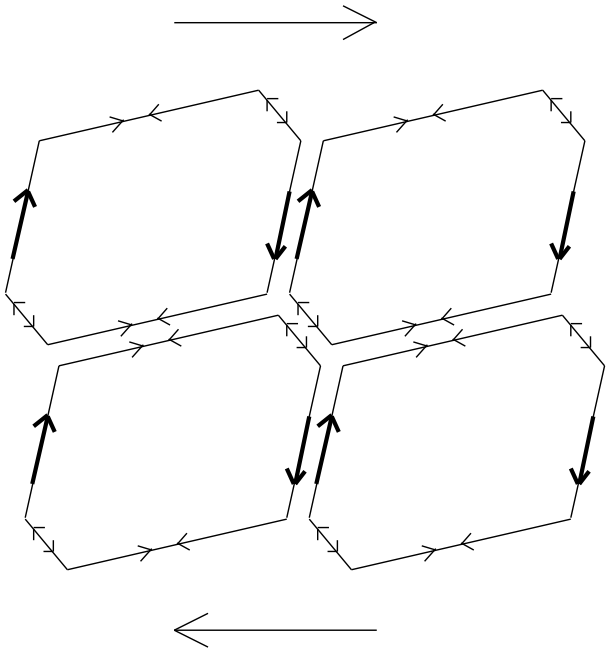

Figure 9. A superposition of Marangoni and Poiseuille flows leads to strong shear in some films (bold arrows) and compression and dilation in others.

but dissipation arising from and water flow, diffusion resistance and surface dilational viscosity. All three processes take place in the "neck" regions connecting the films to the borders. (It should be noted that in this mechanism there is a singular limit for $d \to 0$, in which the slow drainage of water out of the pulled film gives a dominant dissipation [17]. So long as d remains finite, this becomes a *nonlinear* effect, which is, at least formally, irrelevant to the limit under discussion.)

The dissipation in the Marginal Regeneration mechanism is estimated as [15] $T\dot{S} = (\eta_W + T/(Dc\Sigma^2) + \kappa/\rho)\dot{\gamma}^2$ where ρ is the size of a neck (somewhere between r and d). Comparison with the Marangoni process described above suggests the latter to be less dissipative for typical foam parameters. An exception is for ultra-dry foams ($d \to 0$) where the Marginal Regeneration mechanism becomes obligatory.

4.7. MODE STRUCTURE

With the above ideas about water and surfactant flux patterns, we can identify the following candidate modes:

Poiseuille Mode: Driven mainly by disjoining pressure; elastic storage modulus increment $\Delta G_P \simeq \Pi_d d/R \simeq \sigma d/(Rr)$; viscosity increment $\Delta\eta_P \simeq \eta_W R/d$, hence relaxation frequency

$$\omega_P = \frac{\Delta G_P}{\Delta \eta_P} \simeq \frac{\sigma d^2}{R^2 d \eta_W} \tag{21}$$

For wet foams (and parameters relating to the small cell biliquid case) $\Delta G_P \ll G_0$, and $\omega_P \simeq 1 - 100$ Hz. For dry foams, $\Delta G_P \simeq G_0$ but $\omega_P \geq 100$ Hz.

Marangoni Mode: Driven mainly by Gibbs elasticity; elastic storage modulus increment $\Delta G_M \simeq E/R$; viscosity increment $\Delta\eta_M \simeq \eta_W R/d + \kappa/R$; relaxation frequency

$$\omega_M = \frac{\Delta G_M}{\Delta \eta_M} \simeq \frac{E}{\eta_W R^2 d + \kappa} \tag{22}$$

For wet foams, $\Delta G_M \simeq G_0$, but $\omega_M \simeq 100 - 1000$ Hz. For dry foams, $\Delta G_M \simeq G_0$ but $\omega_M \simeq 100$ Hz. Note that in circumstances where Marginal Regeneration prevails (instead of the Marangoni mode), this again gives $\Delta G \simeq G_0$ but $\omega \geq 1000$ Hz.

4.8. BOTTOM LINE

As summarised above, the authors of Ref. [15] did not find a candidate mode which combines both a reasonable amplitude (ΔG of order 0.1 G_0, say) with a low characteristic frequency ($\omega < 1$ Hz). Obviously the analysis is not complete, nor quantitative. Therefore, we do not categorically rule out slow relaxation modes associated with foam-specific dynamics; but this approach does not look promising. It at least seems worthwhile to seek other, more general, mechanisms for slow relaxations. This idea is also motivated by similarities in the rheology of many soft materials.

5. SOFT GLASSY RHEOLOGY

5.1. SOFT GLASSY MATERIALS

The class of materials whose (low frequency) rheology is very similar to that of foams and emulsions is actually quite large; clay slurries, pastes, dense multilamellar vesicles and colloidal glasses are just a few examples [5, 18, 19, 20, 21, 22, 23]. Their elastic (G') and loss (G'') moduli often depend only weakly on frequency ω, with G'' being typically between one and two orders of magnitude smaller than G'. In fact G'' often shows no sign of decreasing to zero for $\omega \to 0$ (as it should if the response is truly linear) even at the lowest frequencies that are accessible experimentally; sometimes it even

seems to rise as ω decreases. These similarities also extend to nonlinear rheology. For example, 'flow curves' of shear stress s versus shear (strain) rate $\dot{\gamma}$ in steady shear flow are generally well described by a relation of the form

$$s = s_Y + c\dot{\gamma}^p \tag{23}$$

with an exponent p between 0.1 and 1. If there is no yield stress ($s_Y = 0$), this is called a 'power law fluid', otherwise a 'Herschel-Bulkley model' [24, 25, 26]. Either way, the materials are 'shear-thinning' in that the apparent viscosity $s/\dot{\gamma}$ decreases as the shear rate $\dot{\gamma}$ increases.

Such qualitative similarities in the rheology of many soft materials suggest an underlying common cause. An obvious candidate, common to all the materials listed above, is (mesoscopic) *structural disorder*. (The importance of this feature has been noted before for specific systems [5, 12, 13, 15, 27, 28], but we feel that its unifying role in rheological modelling has not been properly appreciated.) In a foam, for example, the droplets are normally arranged in a disordered fashion rather than as a regular, crystalline array. The latter would give a lower free energy, and the disordered state is therefore only *metastable*. The *dynamics* of transitions between such metastable states will be *slow*, because typical energy barriers for rearrangements of droplets are much greater than $k_{\rm B}T$. Qualitatively, the same features are found in all the other materials that we have mentioned. More importantly, they are very close to what we normally refer to as a *glass* (except that the disorder there is on a molecular scale). We express this similarity by referring to the class of materials, that we now consider, as "soft glassy materials" (SGM) [29]; the "soft" is added to emphasise that they deform and flow easily, in contrast to many ordinary glasses.

5.2. BOUCHAUD'S GLASS MODEL

We are aiming for a phenomenological model that can explain the main features of SGM rheology (both linear and nonlinear) as described above. To apply to a broad range of SGMs, such a model needs to be reasonably generic. It should therefore incorporate only a minimal number of features common to all SGMs, leaving aside as much system specific detail as possible. We start with the 'glassiness', i.e., the effects of structural disorder and metastability. An intuitive picture of a glass is that it consists of local 'elements' (we will be more specific later) which are trapped in 'cages' formed by their neighbours so that they cannot move. Occasionally, however, a rearrangement of the elements may be possible, due to thermal activation, for example. This idea was formalised into an effective one-element model by Bouchaud (see Refs. [30, 31], where references to earlier work on similar

models can also be found): an individual element 'sees' an energy landscape of traps of various depths E; when activated, it can 'hop' to another trap.

Bouchaud assumed that such hopping processes are due to thermal fluctuations. In SGMs, however, this is unlikely as $k_{\mathrm{B}}T$ is very small compared to typical trap depths E (see later). We assume instead that the 'activation' in SGMs is due to *interactions*: a rearrangement somewhere in the material can propagate and cause rearrangements elsewhere. In a mean-field spirit we represent this coupling between elements by an *effective temperature* (or noise level) x. This idea is fundamental to our model.

We can now write an equation of motion for the probability of finding an element in a trap of depth E at time t:

$$\frac{\partial}{\partial t}P(E,t) = -\Gamma_0 e^{-E/x}\,P(E,t) + \Gamma(t)\,\rho(E) \tag{24}$$

In the first term on the r.h.s., which describes elements hopping out of their current traps, Γ_0 is an attempt frequency for hops, and $\exp(-E/x)$ is the corresponding activation factor. The second term represents the state of these elements directly after a hop. Bouchaud made the simplest possible assumption that the depth of a new trap is completely independent of that of the old one; it is simply randomly chosen from some distribution of trap depths $\rho(E)$. The rate of hopping into traps of depth E is then $\rho(E)$ times the overall hopping rate, given by

$$\Gamma(t) = \Gamma_0 \left\langle e^{-E/x} \right\rangle_P = \Gamma_0 \int e^{-E/x}\,P(E,t)\,dE \tag{25}$$

Bouchaud's main insight was that the model (24) can describe a glass transition *if the density of deep traps has an exponential tail*, $\rho(E) \sim \exp(-E/x_{\mathrm{g}})$, say. Why is this? The steady state of eq. (24), if one exists, is given by $P_{\mathrm{eq}}(E) \sim \exp(E/x)\rho(E)$; the Boltzmann factor $\exp(E/x)$ (no minus here because trap depths are measured from zero *downwards*) is proportional to the average time spent in a trap of depth E. At $x = x_{\mathrm{g}}$, it just cancels the exponential decay of $\rho(E)$, and so the supposed equilibrium distribution $P_{\mathrm{eq}}(E)$ tends to a constant for large E; it is not normalisable. This means that, for $x \leq x_{\mathrm{g}}$, the system does not have a steady state; instead, it 'ages' by evolving into deeper and deeper traps [30, 31]. We therefore identify $x = x_{\mathrm{g}}$ as the *glass transition* of the model (24). In the following, we choose energy units such that this transition occurs at $x = x_{\mathrm{g}} = 1$.

We now have a candidate model for describing the glassy features of SGM. Its main advantage is that it is simple. Its disadvantages are: (i) It has no spatial degrees of freedom, hence cannot describe flow—this we shall fix in a moment. (ii) The assumption of an exponentially decaying $\rho(E)$ is rather arbitrary in our context. It can be justified in systems with

'quenched' (i.e., fixed) disorder, such as spin glasses, using so-called 'extreme value statistics' [32], but it is not obvious how to extend this argument to SGM. (iii) The exponential form of the activation factor in (24) was chosen by analogy with thermal activation. But x describes noise arising from interactions, so this analogy is by no means automatic, and functional forms other than exponential could also be plausible. In essence, we view (ii) *together with* (iii) as a phenomenological way of describing a system with a glass transition. We now ask how such a system will flow.

5.3. MODEL FOR SGM RHEOLOGY

To describe deformation and flow, we now incorporate strain degrees of freedom into the model [29]. As our 'elements' we take *mesoscopic regions* of our SGM. By mesoscopic we mean that these regions must be (i) small enough for a macroscopic piece of material to contain a large number of them, allowing us to describe its behaviour as an *average* over elements; and (ii) large enough so that deformations on the scale of an element can be described by an elastic strain variable. For a single droplet in a foam, for example, this would not be possible because of its highly non-affine deformation; in this case, an element should therefore be at least a few droplet diameters across. We choose the size of the elements as our unit length (to avoid cumbersome factors of element volume in the expressions below).

We denote by l the local shear strain of an element (more generally, the deformation would have to be described by a tensor, but we choose a simple scalar description). This is measured from the *nearest equilibrium configuration of the element*, i.e., the one it would relax to if in complete isolation and without external stresses. When an element is deformed, l will first increase from zero. Assuming the deformation in this regime to be elastic, there will be a local shear stress $s = kl$; k is an appropriate elastic constant, which we take to be the same for all elements. On further deformation, however, the element must eventually yield and rearrange into a new equilibrium configuration; the local strain l is then again zero. This happens when the elastic strain energy $\frac{1}{2}kl^2$ approaches a typical *yield energy* E; due to the disordered structure of the material, the value of this yield energy will in general be different for each element. We can view such yielding events as 'hops' out of a trap (or potential well), and identify the yield energy E with the trap depth. As before, we assume that yields (hops) are activated by interactions between different elements, resulting in an effective temperature x. The activation barrier is now $E - \frac{1}{2}kl^2$, the difference between the typical yield energy and the elastic energy already stored in the element.

We haven't as yet specified how elements behave between rearrangements. The simplest assumption is that their strain changes along with the macroscopically imposed strain γ. This means that, yielding events apart, the *shear rate* is homogeneous throughout the material; on the other hand, the local strain l and stress s are inhomogeneous because different elements yield at different times. We therefore now need to know the joint probability of finding an element with a yield energy E *and* a local strain l to describe the state of the system. An appropriate model for this was set up in Ref. [29]; within the model, the probability evolves in time according to

$$\frac{\partial}{\partial t}P(E,l,t) = -\dot{\gamma}\frac{\partial}{\partial l}P - \Gamma_0\, e^{-(E-\frac{1}{2}kl^2)/x}\, P + \Gamma(t)\,\rho(E)\delta(l) \qquad (26)$$

The first term on the r.h.s. describes the motion of the elements between rearrangements, with a local strain rate equal to the macroscopic one, $\dot{l} = \dot{\gamma}$. The interaction-activated yielding of elements is reflected in the second term. The last term incorporates two assumptions about the properties of an element just after yielding: It is unstrained ($l = 0$; this assumption can be relaxed without qualitative changes to our results) and has a new yield energy E randomly chosen from $\rho(E)$, i.e., uncorrelated with its previous one. Finally, the total yielding rate is given by the analogue of (25),

$$\Gamma(t) = \Gamma_0 \left\langle e^{-(E-\frac{1}{2}kl^2)/x} \right\rangle_P = \Gamma_0 \int e^{-(E-\frac{1}{2}kl^2)/x}\, P(E,l,t)\, dE\, dl \qquad (27)$$

Eq. (26) tells us how the state of the system, described by $P(E,l,t)$, evolves for a given imposed macroscopic strain $\gamma(t)$. What we mainly care about is of course the rheological response, i.e., the macroscopic stress. This is given by the average of the local stresses

$$s(t) = k\,\langle l \rangle_P \equiv k \int l\, P(E,l,t)\, dE\, dl \qquad (28)$$

In the absence of yielding events, the equation of motion (26) then predicts a purely elastic response: $\Delta s \equiv s(t) - s(t') = k\Delta\gamma$. This is a consequence of our assumption that in between rearrangements, the response of each individual element is purely elastic. In reality, there are also viscous contributions; in foams, these are due to the flow of water and surfactant caused by the deformation of the elements. In the low frequency regime of interest to us, such viscous effects are insignificant (see Section 4) and can be neglected. At high frequencies, this is no longer true and the model (26,28) would have to be modified appropriately to yield sensible predictions.

With (26,28), we now have a minimal model for the (low frequency) rheology of SGM: It incorporates both the 'glassy' features arising from

structural disorder (captured in the distribution of yield energies E and local strains l) and the 'softness': for large macroscopic strains, the material flows because eventually all elements yield. One interesting consequence of this is that 'flow interrupts aging': Above, we saw that below the glass transition ($x < 1$), the system evolves into deeper and deeper traps; it ages. In the presence of steady shear flow ($\dot{\gamma} = \text{const}$), however, this doesn't happen: As the local strain l increases with the macroscopic one, the activation barrier $E - \frac{1}{2}kl^2$ of any element decreases to zero in a finite time, for any trap depth E. The system can therefore not get stuck in progressively deeper traps; aging is 'interrupted' [33] and ergodicity is restored.

5.4. PREDICTIONS FOR LINEAR RHEOLOGY

We now summarise the predictions [29] of the model defined by (26,28) for the linear (shear) rheology of SGM. We choose units for energy and time such that $x_g = \Gamma_0 = 1$. We also set $k = 1$, which can always be achieved by a rescaling of the strain variables γ and l. In these units, typical yield strains $\sqrt{2E/k}$ are of order one. Finally, for the density of yield energies ('trap depths') we assume the simplest form with an exponential tail, $\rho(E) = \exp(-E)$. The only parameter that distinguishes between different systems is then the effective noise temperature x. Note that this is not a parameter that we can easily tune from the outside; rather, we expect it to be determined self-consistently by the interactions in the system. This should be borne in mind when we use expressions like "as x increases/decreases" below.

The complex linear modulus predicted by the model [29] turns out to be rather simple:

$$G^*(\omega) = \left\langle \frac{i\omega\tau}{i\omega\tau + 1} \right\rangle_{\text{eq}} \tag{29}$$

This an average over Maxwell modes with relaxation times τ. The distribution of τ follows from the equilibrium distribution of energies, $P_{\text{eq}}(E) \sim \exp(E/x)\rho(E)$. Here τ is given by $\tau = \exp(E/x)$, the 'lifetime' (time between rearrangements) of an element with yield energy E, and this leads to a power-law relaxation time distribution $P_{\text{eq}}(\tau) \sim \tau^{-x}$ (for $\tau \geq 1$). As x decreases towards the glass transition, the long-time tail of the spectrum becomes increasingly dominant and causes anomalous low frequency behaviour of the moduli:

$$\begin{array}{lllll} G'' & \sim & \omega & \text{for } 2 < x, & \sim \omega^{x-1} \quad \text{for } 1 < x < 2 \\ G' & \sim & \omega^2 & \text{for } 3 < x, & \sim \omega^{x-1} \quad \text{for } 1 < x < 3 \end{array} \tag{30}$$

These are illustrated in Fig. 10. The main point to note is that for $1 < x < 2$, i.e., not too far from the glass transition, G' and G'' vary as the same power

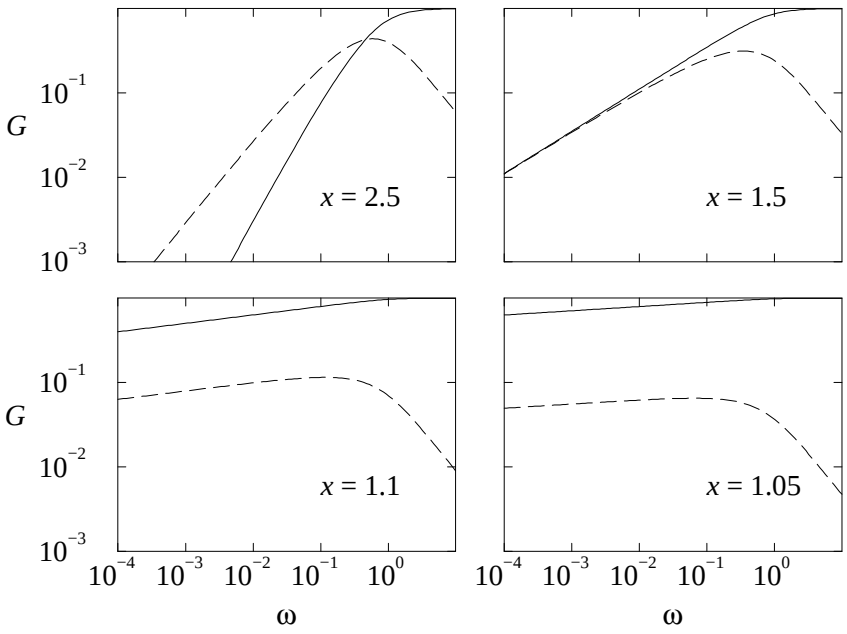

Figure 10. Linear moduli G' (solid line) and G'' (dashed) vs frequency ω at various noise temperatures x above the glass transition.

of frequency (ω^{x-1}); their ratio is therefore constant. Furthermore, as we approach the glass transition ($x \to 1$), this power law becomes increasingly 'flat'. These predictions of the model are compatible with many experimental results [5, 18, 19, 20, 23].

The above linear results only apply for $x > 1$, where there is a well defined equilibrium state around which small perturbations can be made. However, if a cutoff $E_{\max}$ on the yield energies is introduced (which is physically reasonable because yield strains cannot be arbitrarily large), an equilibrium state also exists for $x < 1$, i.e., below the glass transition. (Strictly speaking, with the cutoff imposed there is no longer a true glass phase; but if the energy cutoff is large enough, its qualitative features are expected to be still present.) One then finds for the low frequency behaviour of the linear moduli:

$$G' \sim \text{const.} \qquad G'' \sim \omega^{x-1} \tag{31}$$

This applies as long as ω is still large compared to the cutoff frequency, $\omega_{\min} = \exp(-E_{\max}/x)$. In this frequency regime, G'' therefore increases

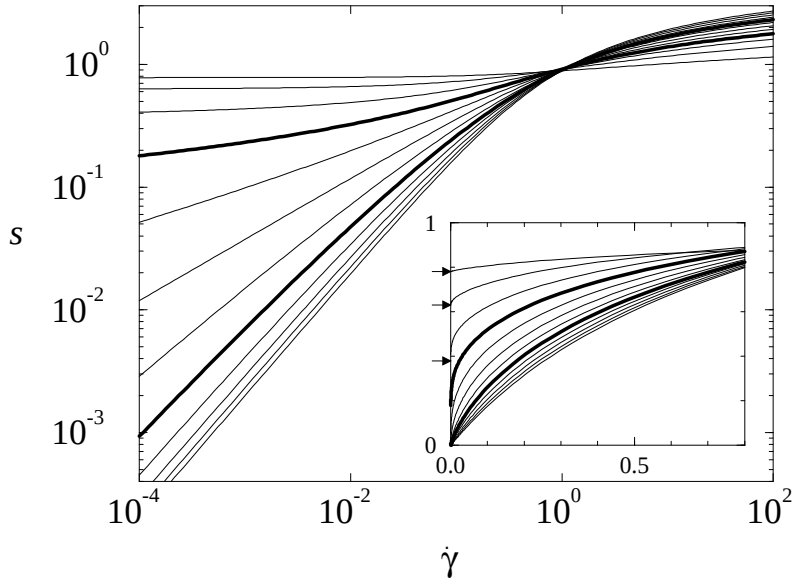

Figure 11. Flow curves: shear stress s vs shear rate $\dot\gamma$, for $x = 0.25, 0.5, \ldots, 2.5$ (top to bottom on left); $x = 1, 2$ are shown in bold. Inset: small $\dot\gamma$ behavior, with yield stresses for $x < 1$ shown by arrows.

as ω decreases, again in qualitative agreement with recent experimental observations [5, 21, 22, 23].

5.5. PREDICTIONS FOR NONLINEAR RHEOLOGY

The model of Ref. [29] can also be used to predict nonlinear rheological features. This is especially important, because arguably the *linear* behaviour described above follows inevitably from the existence of a power law distribution of relaxation times: if we were only interested in the linear regime, it would be simpler just to postulate such a power law! But in fact, an exact (scalar) 'constitutive equation' relating the stress at a given time to the strain history up to that point can be derived [34]. Therefore the model allows one to probe the nonlinear regime in detail.

Here, we only discuss results for the flow curves, i.e., shear stress s vs shear rate $\dot\gamma$ in steady flow (Fig. 11). For high shear rates, strong shear thinning is observed for all x; the stress increases only very slowly with $\dot\gamma$ as $s \sim (x \ln \dot\gamma)^{1/2}$. More interesting is the low shear rate ($\dot\gamma \ll \Gamma_0 = 1$)

behaviour, where three different regimes can be distinguished. (i) For $x > 2$, i.e., far above the glass transition, the behaviour is Newtonian, $s = \eta\dot{\gamma}$. The viscosity, which is simply the average relaxation time, diverges as $x \to 2$ (i.e., at *twice* the glass transition 'temperature'). This signals the onset of a new regime: (ii) For $1 < x < 2$, one has a power law fluid, $s \sim \dot{\gamma}^{x-1}$. The exponent decreases smoothly from 1 to 0 as the glass transition is approached. (iii) In the glass phase ($x < 1$), finally, there is a nonzero yield stress (as one would intuitively expect for a glass). This shows a linear onset, $s_Y \sim 1 - x$, as x decreases below the glass transition temperature. Beyond yield, the stress again increases as a power law, $s - s_Y \sim \dot{\gamma}^{1-x}$. The behaviour of our model in regimes (ii) and (iii) therefore matches respectively the power-law fluid [24, 25, 26] and Herschel-Bulkeley [24, 25] scenarios as used to fit the experimental nonlinear rheology of many SGMs.

5.6. INTERPRETATION OF MODEL PARAMETERS

Our model for SGM captures important rheological features that have been observed in a large number of experiments, at least in the region around a 'glass transition'. Using a mean-field (one element) picture, it is also simple enough to be generic. The main challenge now is the interpretation of the model parameters, namely, the 'effective noise temperature' x and the 'attempt frequency' Γ_0. To answer these questions, we should really start from a proper model for the coupled nonlinear dynamics of the 'elements' of a SGM and then derive our present model within some approximation scheme. At present, we do not know how to do this.

We can nevertheless interpret the activation factor $\exp[-(E - \frac{1}{2}kl^2)/x]$ in (26) as the probability that (within a given time interval of order $1/\Gamma_0$) an element yields due to a 'kick' from a rearrangement elsewhere in the material. Therefore x is the typical activation energy available from such kicks. But while kicks can *cause* rearrangements, they also *arise* from rearrangements (whose effects, due to interactions, propagate through the material). So there is no separate energy scale for kicks: Their energy must of the order of the energies released in rearrangements, i.e., of the order of typical yield energies E. In our units, this means that x should be of order unity. Note that this is far bigger than what we would estimate if x represented true thermal activation. For example, the activation barrier for the simplest local rearrangement in a foam (a T1 or neighbour-switching process) is of the order of the surface energy of a single droplet; this sets our basic scale for the yield energies E. Using typical values for the surface tension and a droplet radius of the order of one μm or greater, we find $E \geq 10^4 k_B T$. In our units $E = O(1)$, so thermal activation would correspond to extremely small values of $x = k_B T \leq 10^{-4}$.

We now argue that x may not only be of order one, but in fact close to one generically. Consider first a steady shear experiment. The rheological properties of a sample freshly loaded into a rheometer are usually not reproducible; they become so only after a period of shearing to eliminate memory of the loading procedure. In the process of loading one expects a large degree of disorder to be introduced, corresponding to a high noise temperature $x \gg 1$. As the sample approaches the steady state, the flow will (in many cases) tend to eliminate much of this disorder [35] so that x will decrease. But, as this occurs, the noise-activated processes will slow down; as $x \to 1$, they may become negligible. Assuming that, in their absence, the disorder cannot be reduced further, x is then 'pinned' at a steady-state value at or close to the glass transition. This scenario, although extremely speculative, is strongly reminiscent of the 'marginal dynamics' seen in some mean-field spin glass models [36].

Consider now the attempt frequency Γ_0. It is the only source of a characteristic timescale in our model (chosen as the time unit above). We have approximated it by a constant value, independently of the shear rate $\dot{\gamma}$; this implies that Γ_0 is not caused by the flow directly. One possibility, then, is that Γ_0 arises in fact from *true* thermal processes, i.e., rearrangements of very 'fragile' elements with yield energies of order $k_{\mathrm{B}}T$. This mechanism can give a plausible rheological time scale *if* one local rearrangement can trigger a long sequence of others [29], as may be the case in foams [12, 28]. Other possible explanations for the origin of Γ_0 include internal noise sources, such as coarsening in a foam, and uncontrolled external noise sources (traffic going past the laboratory where the rheological measurements are performed, for example). The rheometer itself could also be a potential source of noise; this would however suggest at least a weak dependence of Γ_0 on the shear rate $\dot{\gamma}$. We cannot at present say which of these possibilities is most likely, nor rule out other candidates. The origin of Γ_0 may not even be universal, but could in fact be system specific.

6. CONCLUSION

These lectures were intended to summarise our current understanding of linear and nonlinear viscoelasticity in foams. The study of the low frequency linear elastic modulus $G'(\omega \to 0)$ is well-established, but, as described in Section 3, there is a clear discrepancy between the predictions of simplistic ordered models (in both two and three dimensions) and the observed volume fraction dependence of this quantity. This is partially explained by the anomalous spring constant between droplets at weak contact (the Morse-Witten effect) but a full explanation also requires disorder. The latter idea was proposed several years ago by Dennis Weaire and others, but

has only recently been implemented in a three dimensional model [13]. The low frequency loss modulus, $G''(\omega)$ is much harder to understand; the data shows a clear anomaly in that, at the lowest attainable frequencies, this quantity appears to be constant or even rising as the frequency is lowered. Attempts to explain this in terms of foam-specific mechanisms were summarised in Section 4. Although the qualitative analysis of surfactant transport that this entails is certainly of some value, the basic conclusion is that there is no obvious candidate among such mechanisms for explaining the anomalous dissipation in foams. Again, one is drawn to *disorder* as a general explanation.

Accordingly in Section 5, we have described a recent phenomenological model for foam rheology. It captures in a simple yet generic way the effect of mesoscopic structural disorder and metastability; these features are shared by many other 'soft glassy materials'. Thus the model can account for the main qualitative features of the rheology, not only of foams, but of other systems such as slurries and pastes which are commonly observed to show weak power law behaviour and/or near constant loss modulus. The model offers an intriguing link between the linear viscoelastic spectrum and the nonlinear flow curves. However, the interpretation of its parameters, notably the 'effective noise temperature' x, remains to be clarified. To do this may require study of a more fundamental model involving strongly coupled degrees of freedom (as undoubtedly are present in soft glassy materials), rather than the mean-field description used so far.

6.1. ACKNOWLEDGEMENTS

We are indebted to our colleagues Martin Buzza, Pascal Hébraud, Francois Lequeux, and David Lu, much of whose joint work is described in Sections 4 and 5. We are especially grateful to Martin Buzza for permission to use Figs. 1–5, 8 and 9 [37], and to Dov Levine for providing Fig. 6.

References

1. L D Landau and E M Lifshitz. *Statistical Physics, Part 1.* Pergamon, Oxford, 1980.
2. H M Princen. *J. Coll. Interf. Sci.*, 71:55, 1979.
3. H M Princen. Rheology of foams and highly concentrated emulsions. 1: Elastic properties and yield stress of a cylindrical model system. *J. Coll. Interf. Sci.*, 91:160–175, 1983.
4. H M Princen and A D Kiss. Rheology of foams and highly concentrated emulsions. 3: Static shear modulus. *J. Coll. Interf. Sci.*, 112:427–437, 1986.
5. T G Mason, J Bibette, and D A Weitz. Elasticity of compressed emulsions. *Phys. Rev. Lett.*, 75:2051–2054, 1995.
6. D M A Buzza and M E Cates. Uniaxial elastic-modulus of concentrated emulsions. *Langmuir*, 10:4503–4508, 1994.
7. M D Lacasse, G S Grest, and D Levine. Deformation of small compressed droplets. *Phys. Rev. E*, 54:5436–5446, 1996.

8. K Brakke. *Exp. Math.*, 1:141, 1992.
9. D C Morse and T A Witten. Droplet elasticity in weakly compressed emulsions. *Europhys. Lett.*, 22:549–555, 1993.
10. S Hutzler and D Weaire. The osmotic-pressure of a 2-dimensional disordered foam. *J. Phys. Cond. Matt.*, 7:L657–L662, 1995.
11. S Hutzler, D Weaire, and F Bolton. The effects of plateau borders in the 2-dimensional soap froth. 3: Further results. *Phil. Mag. B*, 71:277–289, 1995.
12. D J Durian. Foam mechanics at the bubble scale. *Phys. Rev. Lett.*, 75:4780–4783, 1995.
13. M D Lacasse, G S Grest, D Levine, T G Mason, and D A Weitz. Model for the elasticity of compressed emulsions. *Phys. Rev. Lett.*, 76:3448–3451, 1996.
14. D Levine. Private communication.
15. D M A Buzza, C Y D Lu, and M E Cates. Linear shear rheology of incompressible foams. *J. Phys. (France) II*, 5:37–52, 1995.
16. S R de Groot and P Mazur. *Non-equilibrium thermodynamics.* Dover Publications, New York, 1984.
17. L W Schwartz and H M Princen. A theory of extensional viscosity for flowing foams and concentrated emulsions. *J. Coll. Interf. Sci.*, 118:201–211, 1987.
18. M R Mackley, R T J Marshall, J B A F Smeulders, and F D Zhao. The rheological characterization of polymeric and colloidal fluids. *Chem. Engin. Sci.*, 49:2551–2565, 1994.
19. R J Ketz, R K Prudhomme, and W W Graessley. Rheology of concentrated microgel solutions. *Rheol. Acta*, 27:531–539, 1988.
20. S A Khan, C A Schnepper, and R C Armstrong. Foam rheology. 3: Measurement of shear-flow properties. *J. Rheol.*, 32:69–92, 1988.
21. P Panizza, D Roux, V Vuillaume, C Y D Lu, and M E Cates. Viscoelasticity of the onion phase. *Langmuir*, 12:248–252, 1996.
22. H. Hoffmann and A. Rauscher. Aggregating systems with a yield stress value. *Coll. Polymer Sci.*, 271:390–395, 1993.
23. T G Mason and D A Weitz. Linear viscoelasticity of colloidal hard-sphere suspensions near the glass-transition. *Phys. Rev. Lett.*, 75:2770–2773, 1995.
24. S D Holdsworth. Rheological models used for the prediction of the flow properties of food products. *Trans. Inst. Chem. Eng.*, 71:139–179, 1993.
25. E Dickinson. *An introduction to food colloids.* Oxford University Press, Oxford, 1992.
26. H A Barnes, J F Hutton, and K Walters. *An introduction to rheology.* Elsevier, Amsterdam, 1989.
27. D Weaire and M A Fortes. Stress and strain in liquid and solid foams. *Adv. Phys.*, 43:685–738, 1994.
28. T Okuzono and K Kawasaki. Intermittent flow behavior of random foams - a computer experiment on foam rheology. *Phys. Rev. E*, 51:1246–1253, 1995.
29. P Sollich, F Lequeux, P Hébraud, and M E Cates. Rheology of soft glassy materials. *Phys. Rev. Lett.*, 78:2020–2023, 1997.
30. J P Bouchaud. Weak ergodicity breaking and aging in disordered-systems. *J. Phys. (France) I*, 2:1705–1713, 1992.
31. C Monthus and J P Bouchaud. Models of traps and glass phenomenology. *J. Phys. A*, 29:3847–3869, 1996.
32. J P Bouchaud and M Mézard. Universality classes for extreme value statistics. LPTENS preprint 97/XX. To be published.
33. J P Bouchaud and D S Dean. Aging on Parisis tree. *J. Phys. (France) I*, 5:265–286, 1995.
34. P Sollich. Exact constitutive equation for soft glassy rheology. In preparation.
35. D Weaire, F Bolton, T Herdtle, and H Aref. The effect of strain upon the topology of a soap froth. *Phil. Mag. Lett.*, 66:293–299, 1992.
36. L F Cugliandolo and J Kurchan. Analytical solution of the off-equilibrium dynamics

of a long-range spin-glass model. *Phys. Rev. Lett.*, 71:173–176, 1993.
37. D M A Buzza. *Theory of Emulsions*. PhD thesis, Cambridge University, 1994.